JGR Biogeosciences

RESEARCH ARTICLE
10.1029/2018JG004903

Quantifying Soil Phosphorus Dynamics: A Data Assimilation Approach

Enqing Hou[1,2], Xingjie Lu[2,3], Lifen Jiang[2], Dazhi Wen[1], and Yiqi Luo[2]

[1]Key Laboratory of Vegetation Restoration and Management of Degraded Ecosystems, South China Botanical Garden, Chinese Academy of Sciences, Guangzhou, China, [2]Center for Ecosystem Science and Society, Northern Arizona University, Flagstaff, AZ, USA, [3]School of Atmospheric Sciences, Sun Yat-sen University, Guangzhou, China

Key Points:
- The dynamics of major soil phosphorus pools were quantified using a data assimilation approach
- Labile phosphorus was transferred more to nonoccluded organic phosphorus and secondary mineral phosphorus than to plants
- Soil pH and organic carbon concentration regulated the competition for phosphorus between plants and soil secondary minerals

Supporting Information:
- Supporting Information S1
- Data Set S1

Correspondence to:
E. Hou and Y. Luo,
enqing.hou@nau.edu;
yiqi.luo@nau.edu

Citation:
Hou, E., Lu, X., Jiang, L., Wen, D., & Luo, Y. (2019). Quantifying soil phosphorus dynamics: A data assimilation approach. *Journal of Geophysical Research: Biogeosciences*, *124*, 2159–2173. https://doi.org/10.1029/2018JG004903

Received 30 OCT 2018
Accepted 17 JUN 2019
Accepted article online 2 JUN 2019
Published online 18 JUL 2019

Author Contributions:
Conceptualization: Enqing Hou, Yiqi Luo
Data curation: Enqing Hou, Xingjie Lu, Yiqi Luo
Formal analysis: Enqing Hou, Xingjie Lu, Yiqi Luo
Funding acquisition: Enqing Hou, Dazhi Wen, Yiqi Luo
Resources: Dazhi Wen, Yiqi Luo
Software: Enqing Hou, Xingjie Lu
Supervision: Yiqi Luo
Validation: Enqing Hou, Xingjie Lu, Lifen Jiang
Visualization: Enqing Hou, Lifen Jiang
Writing - original draft: Enqing Hou
Writing – review & editing: Xingjie Lu, Lifen Jiang, Dazhi Wen, Yiqi Luo

Abstract The dynamics of soil phosphorus (P) control its bioavailability. Yet it remains a challenge to quantify soil P dynamics. Here we developed a soil P dynamics (SPD) model. We then assimilated eight data sets of 426-day changes in Hedley P fractions into the SPD model, to quantify the dynamics of six major P pools in eight soil samples that are representative of a wide type of soils. The performance of our SPD model was better for labile P, secondary mineral P, and occluded P than for nonoccluded organic P (Po) and primary mineral P. All parameters describing soil P dynamics were approximately constrained by the data sets. The average turnover rates were labile P 0.040 g g^{-1} day^{-1}, nonoccluded Po 0.051 g g^{-1} day^{-1}, secondary mineral P 0.023 g g^{-1} day^{-1}, primary mineral P 0.00088 g g^{-1} day^{-1}, occluded Po 0.0066 g g^{-1} day^{-1}, and occluded inorganic P 0.0065 g g^{-1} day^{-1}, in the greenhouse environment studied. Labile P was transferred on average more to nonoccluded Po (transfer coefficient of 0.42) and secondary mineral P (0.38) than to plants (0.20). Soil pH and organic C concentration were the key soil properties regulating the competition for P between plants and soil secondary minerals. The turnover rate of labile P was positively correlated with that of nonoccluded Po and secondary mineral P. The pool size of labile P was most sensitive to its turnover rate. Overall, we suggest data assimilation can contribute significantly to an improved understanding of soil P dynamics.

Plain Language Summary Plant growth in terrestrial ecosystems is affected by the supply of phosphorus in the soil, which is itself determined by the amount of phosphorus in the soil that is soluble in water and the rates of changes to it from other forms of phosphorus in the soil. While the amount of water soluble P in the soil is easy to quantify, it is a challenge to quantify the rates of change between the forms of phosphorus in the soil. We showed that data assimilation, a data-model fusion approach, can quantify these rates of change. Some of these were quantified here for the first time, although in a greenhouse environment. We provided a novel approach to quantify the changes of the forms of phosphorus in the soil. This will ultimately contribute to the accurate management of phosphorus fertilizers in agricultural lands and the accurate estimation of phosphorus limitation on plant growth in natural terrestrial ecosystems.

1. Introduction

The dynamics of phosphorus (P) in the soil directly control its bioavailability (George et al., 2018; Hou et al., 2016; Vitousek et al., 2010), which further affects many key functions (e.g., crop production and carbon [C] sequestration) of terrestrial ecosystems (Augusto et al., 2017; George et al., 2018; Penuelas et al., 2013; Wang et al., 2010). Hence, there is a growing demand to incorporate the P cycle into earth system models, to improve predictions for crop production and terrestrial C sequestration under future global change scenarios (Reed et al., 2015; Roy et al., 2016; Sun et al., 2017; Wang et al., 2010). To achieve this goal, we need to quantify soil P dynamics (Helfenstein, Tamburini, et al., 2018; Reed et al., 2015; Sun et al., 2017), which remains a challenge (Helfenstein, Jegminat, et al., 2018; Helfenstein, Tamburini, et al., 2018).

Soil P dynamics mainly includes sorption/desorption, precipitation/dissolution, mineralization/immobilization, weathering, and solid-phase P transformations such as solid-phase diffusion, penetration, and recrystallization (Barrow, 1983; Frossard et al., 2000; Gama-Rodrigues et al., 2014; Hou et al., 2016; Tiessen & Moir, 2007; Vitousek et al., 2010). Among these, fast soil P transformations such as sorption/desorption and mineralization/immobilization have been much studied, because current

approaches are able to quantify soil P dynamics usually within a growing season (Achat, Bakker, et al., 2010; Barrow, 1983; George et al., 2018). For example, isotopic dilution technique, which is considered the most reliable approach to study soil P dynamics, can quantify soil P dynamics successfully at time scales from days to a growing season but hardly at longer time scales, due to the short half-lives of ^{33}P (25.3 days) and ^{32}P (14.3 days; Achat, Bakker, et al., 2010; Bünemann, 2015; Chen et al., 2003; Helfenstein, Jegminat, et al., 2018). The turnover rates of slow-cycling soil inorganic P pools such as second mineral P and primary mineral P have recently been approximated using a combination of sequential extraction with P *K*-edge X-ray absorption spectroscopy and isotopic methods (^{33}P and ^{18}O in phosphate), in Hawaii, United States (Helfenstein, Tamburini, et al., 2018). The wide application of this approach, however, is limited by its use of radioactive isotopes and expensive equipment such as an X-ray absorption near edge spectroscopy and an isotopic ratio mass spectrometer.

Sequential extraction approach has been one of the most common ways to study soil P dynamics, due to its low operational cost and practical feasibility, with the procedure of Hedley et al. (1982) and its modifications as the most commonly used one (Condron & Newman, 2011; Hedley et al., 1982; Hou, Tan, et al., 2018; Hou, Wen, et al., 2018; Hou, Chen, et al., 2018; Tiessen & Moir, 2007). In general, the Hedley P fractionation procedure sequentially removes soil inorganic P (Pi) and organic P (Po) fractions with decreasing solubility or mobility using a series of chemical reagents (Hedley et al., 1982; Tiessen & Moir, 2007). Previous applications of soil P fractionation techniques have provided valuable insights into soil P dynamics, for example, revealing the changes in soil P forms and bioavailability with soil development (Cross & Schlesinger, 1995; Vitousek et al., 2010). Some studies have also applied a regression or path analysis approach to explore the pathways of transformations between soil P pools (Gama-Rodrigues et al., 2014; Hou et al., 2016; Hou, Chen, et al., 2018; Tiessen et al., 1984), providing qualitative or semiquantitative information about soil P dynamics. However, a quantitative understanding of this dynamics is required for the precise management of agricultural soil P availability and reliable predictions about terrestrial ecosystems under global change scenarios (Reed et al., 2015; Roy et al., 2016; Sun et al., 2017).

Data assimilation is a data-model fusion method that combines a model with the data in a rigorous way to constrain the parameters of the model and the states of the system, identify the model error, and improve ecological prediction (Luo et al., 2011; Luo et al., 2016; Niu et al., 2014). It has been successfully used to quantify terrestrial C dynamics, with a combination of process-based C cycle models and field or laboratory measurements of C pools and fluxes (Liang et al., 2015; Luo et al., 2016; Niu et al., 2014). Since the dynamics of soil P is also based on pools and fluxes, a data assimilation analysis of soil P fraction data is potentially able to quantify this dynamics and thus contribute to an improved understanding of soil P dynamics. Yet no study has applied such an approach to quantify soil P dynamics, despite the numerous soil P fraction measurements in the literature (Hou, Tan, et al., 2018; Negassa & Leinweber, 2009). The data assimilation approach is potentially superior to other currently available techniques in quantifying soil P dynamics in several ways. It can use the existing multiple sources of diverse observations (e.g., soil P pool size and plant P uptake), simultaneously quantify the rates of all major soil P processes and provide information about the uncertainties of the parameters related to soil P (Luo et al., 2011; Luo et al., 2016; Niu et al., 2014). And it may be particularly useful to quantify the dynamics of slow-cycling soil P pools (e.g., soil occluded P), which can hardly be achieved by any currently available experimental technique (Helfenstein, Tamburini, et al., 2018).

This study aims to explore whether a data assimilation analysis of soil P fractions can quantify soil P dynamics and contribute to an improved understanding of it. With this aim, we first built a process-based soil P dynamics (SPD) model. Then we assimilated eight data sets of temporal changes in Hedley P fractions (Hedley et al., 1982) into the SPD model, to quantify the dynamics of the major soil P pools. Finally, we linked our estimates to plant P uptake and key soil properties such as soil pH and organic C concentration, to examine the effects of the properties of the plants and soil on soil P dynamics.

2. Materials and Methods

As stated above, one main purpose of this study was to examine the potential of data assimilation in quantifying soil P dynamics. Theoretically, all soil P fraction data can yield information about soil P dynamics. However, low-frequency (e.g., single time) measurements of soil P fractions usually reveal small temporal

Table 1
Basic Physiochemical Properties of the Eight Soils Studied

Soil property	Unit	Honouliuli	Lualualei	Nohili	Paaloa	Wahiawa	Kapaa	Leilehua	Mahana
Soil order		Vertisols	Vertisols	Mollisols	Oxisols	Oxisols	Oxisols	Ultisols	Oxisols
Total P	g/kg	1840	2098	815	596	528	1722	699	1327
Extractable P	mg/kg	26.3	31.9	3.2	1.1	1.6	2.5	1.2	15.8
pH		7.26	7.65	7.44	5.05	5.05	4.92	4.66	4.31
Organic C	g/kg	16.6	4.1	17.1	40.0	35.8	45.6	44	36.7
Exchange cation	$cmol_c/kg$	30.6	106.8	109.5	5.5	4.1	3.8	1.0	1.4
Fe_{ox}	g/kg	3.4	3.82	11.8	7.48	3.27	4.54	6.56	5.7
Al_{ox}	g/kg	1.43	2.94	4.32	2.98	3.65	5.61	6.5	12.81
Sand	g/kg	56.5	49.9	26.8	53.8	20.4	91.5	17.0	146.1
Silt	g/kg	363.6	161.7	166.6	205.4	84.6	383.4	120.2	367.6
Clay	g/kg	580.0	788.4	806.6	740.8	895.0	525.1	862.9	486.3

Note. Extractable P is inorganic P extracted by 0.5 M $NaHCO_3$. Fe_{ox} and Al_{ox} are the concentrations of Fe and Al, respectively, extracted by a mixture of ammonium oxalate and oxlic acid.

changes in soil P fractions and contain very limited information about soil P dynamics (Luo et al., 2009; Luo et al., 2016). Soil P fractions determined using different fractionation procedures are not directly comparable (Hou, Tan, et al., 2018). Therefore, we preferred consistent and frequent measurements of the P fractions in a group of soils with a wide variety of physiochemical properties. By searching the literature, we found data sets in Guo et al. (2000) meeting our requirements well. This is because Guo et al. (2000) reported consistent (i.e., using the same fractionation procedure) and frequent (i.e., seven or eight times) measurements of the P fractions of eight soils that represent eight soil series and four of the twelve major USDA soil types (Table 1). In addition, most soil P fractions changed substantially or significantly during the study period (Figure S1; Guo et al., 2000). Such data sets are more likely to constrain soil P dynamics, and the soil samples are representative of a wide type of soils. A less desirable feature of these data sets is that they derived from experiments performed in a greenhouse, where the soil P pools could have higher turnover rates than in the field. This will be discussed in section 4.

2.1. Greenhouse Experiment

Guo et al. (2000) described in detail the experimental design, cropping, sampling and preparation of the soils, and determination of the P fractions and physiochemical properties of the soils. In general, they used crops to remove labile P from eight soils to trigger changes in the P fractions in these soils over a total of 14 cropping periods. After every two croppings, they sampled small amounts of the soils to determine the soil P fractions.

Guo et al. (2000) planted crops in plastic pots (18 cm in diameter and 30-cm deep) in a greenhouse. For croppings 1 to 10, 13, and 14, they planted corn seeds (*Zea mays* L.) and harvested the corn after 28 days of growth. For croppings 11 and 12, they planted soybean seeds (*Glycine max* [L.] Merr.) and harvested the soybeans after 45 days of growth. They also carried out several treatments (e.g., N fertilization and irrigation) to facilitate intensive uptake of P from the soils. They set a randomized complete block with three replicates of each type of soil.

Guo et al. (2000) took a 2-g soil sample from each pot before the first planting and after croppings 2, 4, 6, 8, 10, 12, and 14 (i.e., 0, 56, 112, 168, 224, 280, 370, and 426 days after the first planting, as used in our data assimilation system) for the determination of the soil P fractions. They determined the soil P fractions using a modified Hedley procedure (Hedley et al., 1982). In brief, they sequentially extracted a 0.5-g soil sample with (1) 30-ml deionized water and one Fe-impregnated strip (2×10 cm^2), (2) 0.5 M $NaHCO_3$ at pH 8.5, (3) 0.1 M NaOH, (4) 1 M HCl, and (5) 5.0-ml concentrated H_2SO_4 and 2 to 3-ml H_2O_2. They determined the inorganic P (Pi) in all five extracts (i.e., the strip-P, $NaHCO_3$-Pi, NaOH-Pi, HCl-P, and residual P fractions) by the method of Murphy and Riley (1962). They determined the total P (P_T) in extracts 2 and 3 by the method of Murphy and Riley (1962) after autoclave digestion to convert Po to Pi with acid ammonium peroxysulfate (Guo et al., 2000). They calculated the organic P in extracts 2 and 3 as the difference between P_T and Pi in these extracts.

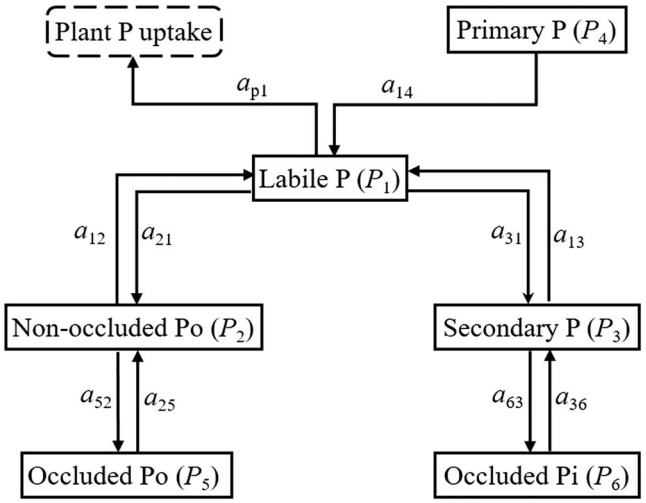

Figure 1. Schematic representation of the soil P dynamics model. Primary P indicates primary mineral P; secondary P indicates secondary mineral P; Pi indicates inorganic P; Po indicates organic P. An "*a*" on an arrow indicates the coefficient of soil P transformation: plant immobilization (a_{p1}), weathering (a_{14}), microbial immobilization (a_{21}), mineralization (a_{12}), sorption/precipitation (a_{31}), desorption/dissolution (a_{13}), and solid-phase transformations (a_{25}, a_{52}, a_{36}, and a_{63}).

2.2. Description of the Model

The soil P dynamics (SPD) model (Figure 1) was modified from the conceptual model of Tiessen et al. (1984) according to the selected data sets. Specifically, the sum of the strip-P and the $NaHCO_3$-Pi was calculated as labile P (P_1 in Figure 1). This is because the strip-P and the $NaHCO_3$-Pi were highly positively correlated ($r = 0.85$, $P < 0.001$, $n = 60$) and changed in similar ways over the course of the experiment (Figure S1 in the supporting information). The sum of the $NaHCO_3$-Po and the NaOH-Po was calculated as nonoccluded Po (P_2 in Figure 1), because of the functional similarity between the two Po fractions (Hou et al., 2016; Tiessen & Moir, 2007). Similarly, as defined by Tiessen et al. (1984), the NaOH-Pi was used as secondary mineral P (P_3 in Figure 1), and the HCl-P was used as primary mineral P (P_4 in Figure 1). The residual P in organic and inorganic forms were defined as occluded Po (P_5 in Figure 1) and occluded Pi (P_6 in Figure 1), respectively (Tiessen et al., 1984). In Guo et al. (2000), the residual P was believed to be composed of but not separated into residual organic P and residual inorganic P. A proportion of occluded P in organic forms (OP_o) was introduced in our study to represent the amounts of occluded Po (calculated as residual P × OP_o) and occluded Pi (calculated as residual P × (1 − OP_o)). The lower/upper bounds and initial value of OP_o (Table S1) were set based on the proportions of organic P in the $NaHCO_3$ and the NaOH extracts, as justified in detail in Text S1.

Our SPD model included all major soil P transformations, as detailed in Figure 1. Plant P uptake during a specific period was calculated as the sum of the decreases in $P_{1\text{-}6}$ during the period. For instance, plant P uptake after cropping 14 was calculated as the difference between the sum of $P_{1\text{-}6}$ at cropping 0 and the same sum after cropping 14. Soil moisture content was maintained near soil available water capacity during the experiment (Guo et al., 2000); therefore, no P leaching was considered in our SPD model. Since this took place in greenhouse environment, no atmospheric P deposition was considered. No leaf litter was likely to be produced during the experiment, because plants were young (≤45 days of growth). Although Guo et al. (2000) did not describe how they harvested the crops, we assumed that they harvested the whole of the plants (i.e., both the aboveground and the belowground parts) without leaving significant amounts of roots in the soil, because they were aimed to remove as much P from the soil as possible to trigger essential changes in the soil P fractions. Hence, no litter production or litter decomposition was considered in our SPD model. Note that if roots were not harvested or if coarse roots were harvested with much of the fine roots left in the soil, a pathway from the plants to nonoccluded Po would need to be considered during modeling.

In reference to the SPD model in Figure 1, soil P dynamics are represented by the following set of balance equations.

$$\begin{cases} \dfrac{dP_1(t)}{dt} = a_{14}P_4(t) + a_{12}P_2(t) + a_{13}P_3(t) - k_1P_1(t) \\ \dfrac{dP_2(t)}{dt} = a_{21}P_1(t) + a_{25}P_5(t) - k_2P_2(t) \\ \dfrac{dP_3(t)}{dt} = a_{31}P_1(t) + a_{36}P_6(t) - k_3P_3(t) \\ \dfrac{dP_4(t)}{dt} = -k_4P_4(t) \\ \dfrac{dP_5(t)}{dt} = a_{52}P_2(t) - k_5P_5(t) \\ \dfrac{dP_6(t)}{dt} = a_{63}P_3(t) - k_6P_6(t) \end{cases} \quad (1)$$

Note that plant P uptake was not listed in equation (1), because it is treated as a soil P flux in the SPD model. Meanwhile, a_{p1} was not used in equation (1), because it can be directly estimated from a_{21} and a_{31} by the following equation:

$$a_{p1} = 1 - a_{21} - a_{31} \tag{2}$$

The set of balance equations (1) can be summarized by the following first-order differential equation:

$$\frac{dP(t)}{dt} = -AKP(t) \tag{3}$$

where A and K are the matrices given by

$$A = \begin{pmatrix} -1 & a_{12} & a_{13} & 1 & 0 & 0 \\ a_{21} & -1 & 0 & 0 & 1 & 0 \\ a_{31} & 0 & -1 & 0 & 0 & 1 \\ 0 & 0 & 0 & -1 & 0 & 0 \\ 0 & 1-a_{12} & 0 & 0 & -1 & 0 \\ 0 & 0 & 1-a_{13} & 0 & 0 & -1 \end{pmatrix}$$

$$K = \mathrm{diag}(k) = \begin{pmatrix} k_1 & 0 & 0 & 0 & 0 & 0 \\ 0 & k_2 & 0 & 0 & 0 & 0 \\ 0 & 0 & k_3 & 0 & 0 & 0 \\ 0 & 0 & 0 & k_4 & 0 & 0 \\ 0 & 0 & 0 & 0 & k_5 & 0 \\ 0 & 0 & 0 & 0 & 0 & k_6 \end{pmatrix}$$

and $P(t) = (P_1(t) \cdot P_2(t) \cdot P_3(t) \cdot P_4(t) \cdot P_5(t) \cdot P_6(t))^T$ is a 6×1 vector describing the sizes of the soil P pools.

Matrix A gives the transfers of P between the individual P pools, as described by the arrows in Figure 1. The elements (a_{ij}) are the P transfer coefficients, representing the fraction of P entering the ith (row) pool from the jth (column) pool. a_{52} is calculated as $1 - a_{12}$; a_{63} is calculated as $1 - a_{13}$; a_{14}, a_{25}, and a_{36} are fixed at 1.0. K is a 6×6 diagonal matrix representing the release rates of six soil P pools (units: g P g^{-1} P day^{-1}; for convenience, g g^{-1} day^{-1} was used in the following), i.e., the amount of P leaving each of the soil P pools per day.

2.3. Model Validation and Data Assimilation

Before the data assimilation analysis, we validated the SPD model with soil P pool measurements at cropping 0 (Table S2) and initial model parameter values (i.e., initial values of $k_{1\text{-}6}$, OP_o, and the as; Table S1). The prior knowledge used to ascertain the initial model parameter values was described in Text S1. The same parameter values were used for all the eight soils studied. In general, the SPD model simulated temporal changes in the soil P pools reasonably well, with a better performance for labile P, secondary mineral P, and occluded P than for nonoccluded Po and primary mineral P (Figure S2 and Table S3).

The performance of the model was quantified by both R^2 of the linear relationship between the measurements (X axis) and the modeled values (Y axis) and the normalized root-mean-square error (NRMSE) for each P pool of each soil. The NRMSE was calculated as

$$\mathrm{NRMSE} = \frac{\sqrt{\frac{1}{N}\sum_{i=1}^{N}\left(Z_i^{\mathrm{sim}} - Z_i^{\mathrm{obs}}\right)^2}}{\bar{y}} \tag{4}$$

where Z_i^{obs} is the ith measurement of a soil P pool, Z_i^{sim} is the corresponding model value, N is the total number of measurements for the soil P pool, and $\bar{y}$ is the average of the N measurements of the soil P pool.

For the data assimilation analysis, we used a probabilistic inversion approach described by Liang et al. (2015) to estimate the parameters describing soil P dynamics. The approach is based on Bayes' theorem:

$$P(\theta|Z) \propto P(Z|\theta)P(\theta) \tag{5}$$

where $P(\theta|Z)$ was the posterior probability density function (PDF) of model parameter θ, $P(Z|\theta)$ was a likelihood function that included information obtained during the greenhouse experiment, and $P(\theta)$ was the

prior knowledge of parameter θ. The prior PDF was specified as the uniform distribution over the range of the specific parameter. The likelihood function $P(Z|\theta)$ was calculated with the assumption that the errors between the observed and the modeled values were independent from each other and followed a multivariate Gaussian distribution with a zero mean:

$$P(Z|\theta) \propto \exp\left\{-\sum_{i=1}^{6}\sum_{t\in obs(Z_i)}\frac{[Z_i(t)-X_i(t)]^2}{2\sigma_i^2(t)}\right\} \quad (6)$$

where $Z_i(t)$ and $X_i(t)$ were the observed and the modeled values of P (either one of the five measured soil P pools or plant P uptake), respectively, and $\sigma_i(t)$ was the standard deviation of the measurement.

The probabilistic inversion was carried out on using the Metropolis-Hasting (M-H) algorithm, which is a Markov Chain Monte Carlo technique (Hastings, 1970) to construct the posterior PDFs of the parameters. Briefly, the M-H algorithm repeats two steps: a proposing step and a moving step. In the proposing step, a new point θ^{new} is generated based on the previously accepted point θ^{old} with a proposal distribution $P(\theta^{new}|\theta^{old})$:

$$\theta^{new} = \theta^{old} + \frac{d(\theta_{max}-\theta_{min})}{D} \quad (7)$$

where θ_{max} and θ_{min} were the maximum and minimum values in the prior range of the given parameter, d was a random variable between −0.5 and 0.5 with a uniform distribution, and D was used to control the proposing step size and was set to 30 in the current study. In the moving step, the new point θ^{new} was tested against the Metropolis criterion to examine if it should be accepted or rejected. Because the initial accepted samples were in the burn-in period, the first half of accepted samples were discarded and only the rest were used to generate posterior PDFs.

Measurement errors of soil P pools were not given in Guo et al. (2000). Instead, they (Table S4) were estimated based on the Fisher's least square deviations given in Guo et al. (2000) and current knowledge of the errors in Hedley P fraction measurements (Condron & Newman, 2011; Tiessen & Moir, 2007). In general, small soil P pools (e.g., primary mineral P in highly weathered soils and labile P) have larger measurement errors than large soil P pools (e.g., primary mineral P in lightly weathered soils and occluded P), due to their ease of loss and/or being contaminated by the previous extract during fractionation (Condron & Newman, 2011; Tiessen & Moir, 2007) and their close proximity to the detection limit of the typically used colorimetric method (Murphy & Riley, 1962). Active soil P pools (e.g., nonoccluded Po) have larger measurement errors than the less active soil P pools (e.g., occluded P), due to their more intense reactions with the chemical reagents used for extraction (Condron & Newman, 2011). The lower/upper bounds and initial value of each parameter (Table S1) were set based on current knowledge of soil P transformations, as justified in Text S1.

To facilitate intensive uptake of P by the crop, Guo et al. (2000) treated all soils with P fertilizers and then incubated the soils for 60 days to allow the P fertilizers to mix well with the P in the soils. Temporal changes in soil P fractions (Figure S1), however, showed that the P fertilizers had not yet mixed well with the P in the soils at cropping 0. To deal with this experimental problem, we estimated the soil P fractions at cropping 0 using a probabilistic inversion approach as described by equation (7). We listed the initial value and range of the proportion of each soil P pool in the total soil P at cropping 0 in Table S2. In general, the initial values were calculated from soil P pool measurements at cropping 0, and the ranges were estimated based on the temporal changes in soil P pools after cropping 0 (Figure S1).

The M-H algorithm was formally run 5 replicates and 500,000 times for each soil to examine the convergence of the parameters. We tested the convergence of the sampling chains by the Gelman-Rubin (*G-R*) diagnostic method to ensure that the within-run variation is roughly equal to the between-run variation.

$$W_i = \frac{1}{K}\sum_{k=1}^{k}\sigma_k^2 \quad (8)$$

$$B_i = \frac{N}{K-1}\sum_{k=1}^{k}\left(\bar{p}^{\cdot,k}-\bar{p}^{\cdot\cdot\cdot}\right)^2 \quad (9)$$

where K is the number of replicates, N is the number of accepted interactions after the burn-in period, $\overline{p}^{\cdot,k}$ and σ_k are the mean and standard deviation of the specific parameter in the kth replicate, and $\overline{p}^{\cdot,\cdot}$ is the mean of the specific parameter over the five replicates. When the Markov chain reaches convergence, GR_i is close to 1.0.

$$GR_i = \sqrt{\frac{W_i(N-1)/N + B_i/N}{W_i}} \tag{10}$$

In this study, the GRs of all parameters of all soils were < 1.10 (Table S5), indicating that all the parameters reached approximate convergence (Brooks & Gelman, 1998).

2.4. Sensitivity Analysis of the Model Parameters

The sensitivity of the modeled soil P pools to the model parameters was analyzed using a first-order approximation method, as described by Gao et al. (2011). For a modeled soil P pool, Z, we first quantified an unconditional variable $V(Z)$ from model output when all parameters p_i in matrices K and A, freely vary over their entire ranges as listed in Table S1. We then estimated the conditional expectation of variable Z for each parameter p_i (for $i = 1, 2, \ldots 11$, i.e. $k_{1\text{-}6}$, a_{21}, a_{31}, a_{12}, a_{13}, OP_o). We randomly selected a value of p_i from a uniform distribution within its prior range p_i^*, as shown in Table S1. We then randomly selected 1000 values for each of the other parameters (p_j: $j \neq i$) from uniform distributions within their prior ranges. From this sample of 1000 parameter sets we estimated a conditional expectation $E\left(Z|p_i = p_i^*\right)$. We repeated this sampling for 100 randomly selected values of p_i and used the results to estimate the variance $V(E(Z|\, p_i))$. Finally, we repeated this procedure for each of p_i (for $i = 1, 2, \ldots 11$).

A sensitivity index S_i was calculated for each parameter p_i (for $i = 1, 2, \ldots 11$), where

$$S_i = \frac{V(E(Z|p_i))}{V(Z)} \tag{11}$$

To compare S_i for all the modeled soil P pools, we normalized S_i by

$$I_i = \frac{S_i}{\sqrt{\sum_{i=1}^{11} S_i^2}} \tag{12}$$

where I_i is the normalized sensitivity index, with a larger value of I_i indicating a greater sensitivity of the soil P pool to the ith parameter. We calculated I_i for all modeled soil P pools.

2.5. Statistical Analysis

We calculated Pearson's correlation coefficients for the model parameters based on 1,000 sets of parameter values that were randomly selected from the second half of accepted samples. The relationships between the Maximum Likelihood Estimates of the parameters and the physiochemical properties of the soil as well as plant P uptake were analyzed using Pearson's correlation and linear regression in SigmaPlot 12.0 (Systat Software, San Jose, CA, United States).

3. Results

The 14 croppings had essentially changed all soil P pools, with labile P changed by −87.8% to −61.0% (a negative value means a decrease and a positive value means an increase, the same below), nonoccluded Po changed by −23.3%–62.2%, secondary mineral P changed by −86.1%–1.5%, primary mineral P changed by −49.3%–216.0%, and occluded P changed by −21.6%–19.7% (Figure 2). Generally, the SPD model simulated well these temporal changes (Figure 2). The relationships between the measured and the modeled soil P pools were mostly significant ($P < 0.05$), with R^2 values generally larger for labile P, secondary mineral P, and occluded P than for nonoccluded Po and primary mineral P (Tables S3). NRMSE was small (<0.3) for all pools of all soils except for primary mineral P of the five highly weathered soils (0.391–1.023; Table S3). This was mainly due to the relatively small amounts of primary mineral P in the five highly weathered

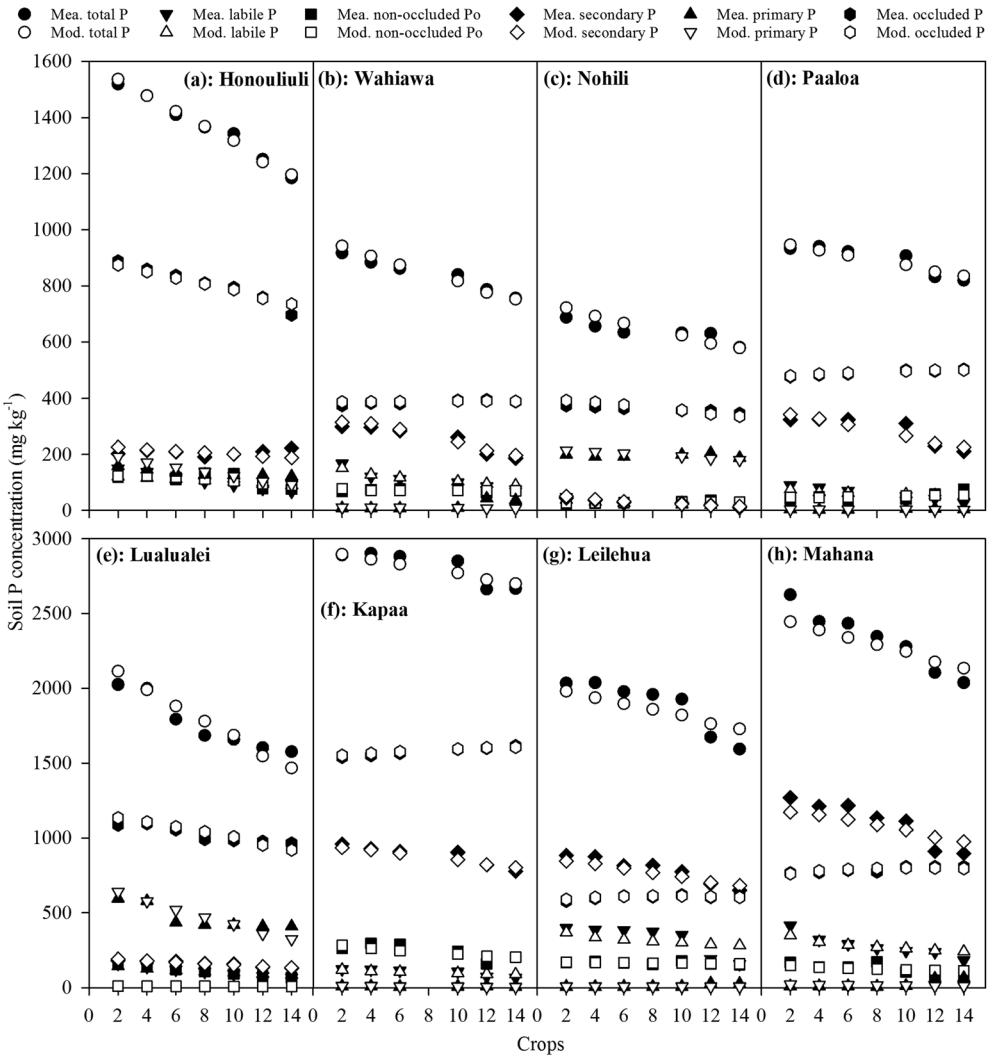

Figure 2. Measured and modeled changes in P pools of the eight soils studied with cropping after data assimilation. The eight soils are Honouliuli (a), Wahiawa (b), Nohili (c), Paaloa (d), Lualualei (e), Kapaa (f), Leilelua (g), and Mahana (h). Secondary P: secondary mineral P; primary P: primary mineral P.

soils (4.3–24.7 mg/kg; Figure S1e). Most of the parameters have one apparent peak in their probability distributions for all soils (Figures S3 and S4).

The turnover rate of labile P was positively correlated to those of nonoccluded Po and secondary mineral P in all soils (average r of 0.54 and 0.63, respectively), and was also positively correlated to the coefficients of transfers from nonoccluded Po and secondary mineral P to labile P in most soils (average r of 0.34 and 0.52, respectively; Tables 2 and S6). The turnover rates of nonoccluded Po and secondary mineral P were positively correlated to their transfers from labile P in all soils (average r of 0.55 and 0.54, respectively; Tables 2 and S6). The coefficient of transfer from labile P to nonoccluded Po was negatively correlated to the coefficient of transfer from labile P to secondary mineral P in all soils (average r of −0.88; Tables 2 and S6).

The amount of labile P was the most sensitive to its turnover rate in all soils (I = 0.81–0.99; Tables 3 and S7). Moreover, it was sensitive to the turnover rate of secondary mineral P in four of the five highly weathered soils (Paaloa [I = 0.30], Kapaa [0.40], Leilehua [0.19], and Mahana [0.54]) and was sensitive to the release rate of primary mineral P in two of the three lightly weathered soils (Honouliuli [0.27] and Nohili [0.15]; Table S7). Nonoccluded Po, secondary mineral P, primary mineral P, and occluded P were sensitive (I > 0.2) to both their own turnover rates and the turnover rate of labile P in most of

Table 2
Coefficients of Correlations Between the Posterior Parameters

Parameter	k_1	k_2	k_3	k_4	k_5	k_6	a_{21}	a_{31}	a_{12}	a_{13}
k_2	**0.54**									
k_3	**0.63**	0.16								
k_4	0.03	−0.01	0.02							
k_5	−0.09	0.18	−0.09	−0.03						
k_6	0.05	0.15	0.46	0.00	−0.01					
a_{21}	−0.10	**0.55**	−0.36	−0.06	0.03	0.12				
a_{31}	0.37	−0.30	**0.54**	0.03	−0.07	−0.06	**−0.88**			
a_{12}	0.34	0.22	0.16	0.00	−0.21	−0.08	0.20	−0.06		
a_{13}	**0.52**	0.28	0.08	−0.02	−0.16	−0.49	−0.22	0.39	0.02	
OP_o	−0.02	0.04	−0.09	−0.05	−0.14	−0.03	−0.11	0.08	−0.06	0.11

Note. Data are average values of eight soils. Absolute values ≥0.50 are shown in bold. Data of each soil are shown in Table S6. For each soil, $n = 1{,}000$. $k_{1\text{-}6}$ are the turnover rates of labile P, nonoccluded Po, secondary mineral P, primary mineral P, occluded Po, and occluded Pi, respectively. a_s are the coefficients of the P transformations described in Figure 1. OP_o is the proportion of occluded Po to occluded P.

the soils (Tables 3 and S7). Occluded P was generally sensitive to all parameters in all soils ($I \geq 0.12$; Tables 3 and S7).

The average turnover rates of the soil P pools were labile P 0.040 g g^{-1} day^{-1}, nonoccluded Po 0.051 g g^{-1} day^{-1}, secondary mineral P 0.023 g g^{-1} day^{-1}, primary mineral P 0.00088 g g^{-1} day^{-1}, occluded Po 0.0066 g g^{-1} day^{-1}, and occluded Pi 0.0065 g g^{-1} day^{-1} (Table 4). Both the turnover and transformation rates of the P pools varied across soils (coefficient of variance of 36%–88%; Table 4). The turnover rate of secondary mineral P was ~4 times higher in the lightly weathered soils (0.044–0.047 g g^{-1} day^{-1}) than in the highly weathered soils (0.006–0.013 g g^{-1} day^{-1}; Table 4). The coefficient of transfer from labile P to plants tended to be higher in the lightly (0.16–0.59, mean 0.34) than the highly weathered soils (0.04–0.020, mean 0.11), while the opposite trend was true for the coefficient of transfer from labile P to secondary mineral P (lightly weathered: 0.06–0.33, highly weathered: 0.31–0.61; Table 4).

The turnover rate of secondary mineral P increased with increasing soil pH ($R^2 = 0.99$, $P < 0.001$; Figure 3a). The coefficient of transfer from labile P to plants also increased with increasing soil pH ($R^2 = 0.53$, $P = 0.042$), with a corresponding decrease in the coefficient of transfer from labile P to secondary mineral P ($R^2 = 0.71$, $P = 0.009$; Figure 3c). The relationships of soil organic C with model parameters were generally opposite to those of soil pH (Figure 3 and Table S8). Plant P uptake decreased with increasing coefficient of transfer from labile P to nonoccluded Po ($R^2 = 0.81$, $P = 0.002$; Figure 4). Neither oxalate extractable Fe nor oxalate extractable Al was significantly related to any of the parameters ($P > 0.05$; Table S8).

Table 3
Normalized Sensitivity Indices of the Model Parameters

Parameter	Labile P	Nonoccluded Po	Secondary mineral P	Primary mineral P	Occluded P
k_1	**0.96**	**0.71**	**0.52**	**0.39**	**0.28**
k_2	0.05	**0.21**	**0.34**	0.17	**0.26**
k_3	0.09	**0.22**	**0.40**	**0.44**	**0.22**
k_4	0.13	0.15	0.12	**0.42**	**0.47**
k_5	0.06	0.07	0.10	0.11	**0.24**
k_6	0.05	0.06	0.08	0.12	**0.22**
a_{21}	0.04	0.17	0.19	0.14	**0.31**
a_{31}	0.04	0.05	0.09	0.13	0.20
a_{12}	0.09	0.09	0.11	0.11	**0.26**
a_{13}	0.05	0.06	0.08	0.09	**0.24**
OP_o	0.04	0.04	0.05	0.09	**0.23**

Note. Data are averaged values of eight soils. Data of each soil are shown in Table S7. Data >0.20 are in bold. See Table 1 for abbreviations.

4. Discussion

The dynamics of the soil P control its P bioavailability, yet it remains a challenge to quantify the dynamics either in the field or in a laboratory or greenhouse environment. This study shows that data assimilation is able to quantify the dynamics of all major soil P pools in a greenhouse environment. The estimated turnover rates of secondary mineral P and primary mineral P were comparable to the previous estimates using isotope dilution and spectroscopic techniques. The estimated soil P transformation rates enabled robustly comparing P transformation rates among soil processes and soils. By linking the estimated parameters to the properties of the soil and the plant P uptake, we identified soil pH and organic C concentration as the key regulators of the competition for P between plants and soil secondary minerals in the plant-soil systems studied.

4.1. Soil P Dynamics and Their Relations to Soil Properties and Plant P Uptake

Previous studies have estimated the turnover rate of solution P in soils worldwide (10^1–10^9 g g^{-1} day^{-1}; Helfenstein, Jegminat, et al.,

Table 4
Maximum Likelihood Estimates of the Model Parameters

Parameter	Unit	Lightly weathered soil			Highly weathered soil					Mean	CV (%)
		Honouliuli	Lualualei	Nohili	Paaloa	Wahiawa	Kapaa	Leilehua	Mahana		
k_1	g g^{-1} day^{-1}	0.040	0.027	0.063	0.048	0.021	0.065	0.024	0.029	0.040	41
k_2	g g^{-1} day^{-1}	0.022	0.096	0.095	0.073	0.043	0.020	0.038	0.019	0.051	60
k_3	g g^{-1} day^{-1}	0.044	0.047	0.047	0.012	0.010	0.013	0.009	0.006	0.023	76
k_4	g g^{-1} day^{-1}	0.00193	0.00187	0.00043	0.00015	0.00022	0.00180	0.00021	0.00041	0.00088	88
k_5	g g^{-1} day^{-1}	0.0077	0.0014	0.0069	0.0067	0.0049	0.0093	0.0073	0.0090	0.0066	36
k_6	g g^{-1} day^{-1}	0.0062	0.0038	0.0055	0.0090	0.0095	0.0025	0.0090	0.0067	0.0065	37
a_{21}	Unitless	0.51	0.08	0.66	0.53	0.49	0.43	0.39	0.30	0.42	38
a_{31}	Unitless	0.33	0.32	0.06	0.38	0.31	0.53	0.47	0.61	0.38	42
a_{p1}	Unitless	0.16	0.59	0.28	0.09	0.20	0.04	0.14	0.09	0.20	82
a_{12}	Unitless	0.97	0.24	0.21	0.23	0.25	0.89	0.73	0.95	0.56	60
a_{52}	Unitless	0.03	0.76	0.79	0.77	0.75	0.11	0.27	0.05	0.44	75
a_{13}	Unitless	0.23	0.30	0.96	0.72	0.84	0.49	0.88	0.76	0.65	40
a_{63}	Unitless	0.77	0.70	0.04	0.28	0.16	0.51	0.12	0.24	0.35	72
OP_o	Unitless	0.28	0.02	0.02	0.02	0.22	0.28	0.21	0.18	0.15	72

Note. See Table 1 for abbreviations. a_{p1} is calculated as 1-a_{21}-a_{31}. a_{52} is calculated as 1-a_{12}. a_{63} is calculated as 1-a_{13}. CV is the coefficient of variance.

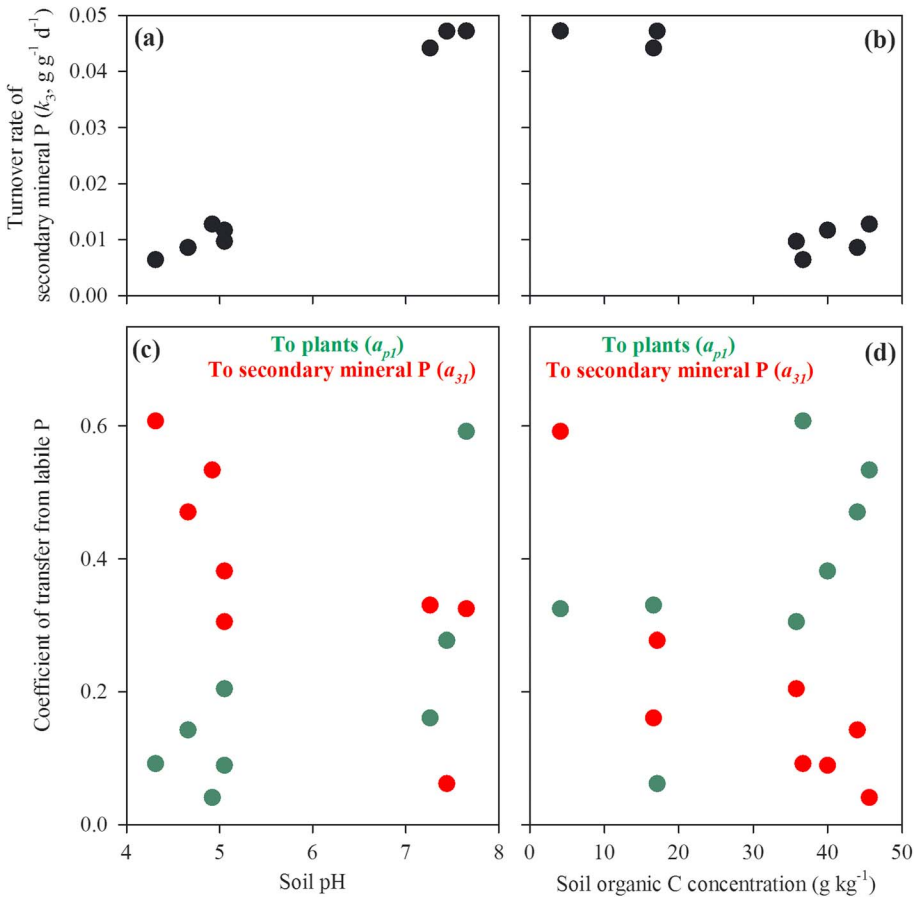

Figure 3. Estimated turnover and transformation rates of soil P pools in relations to key soil properties. The turnover rate of secondary mineral P versus soil pH (a; $R^2 = 0.99$, $P < 0.001$) and organic C concentration (b; $R^2 = 0.87$, $P = 0.001$). The coefficients of transfers from labile P to plants (green; $R^2 = 0.53$, $P = 0.042$) and secondary mineral P (red; $R^2 = 0.71$, $P = 0.009$) versus soil pH (c). The coefficients of transfers from labile P to plants (green; $R^2 = 0.56$, $P = 0.034$) and secondary mineral P (red; $R^2 = 0.38$, $P = 0.106$) versus organic C concentration (d).

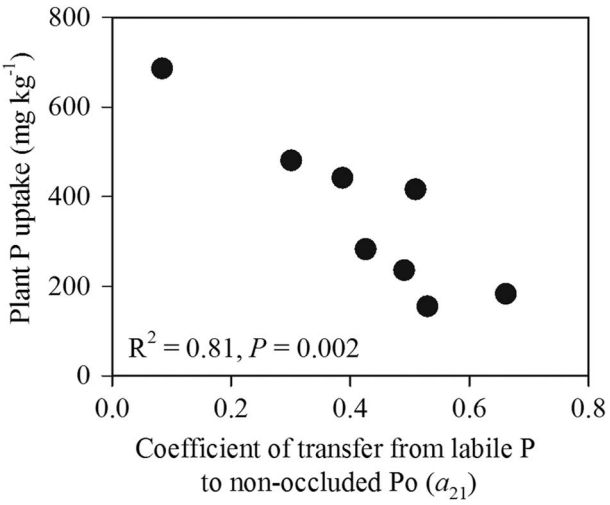

Figure 4. Plant P uptake in relation to the coefficient of transfer from labile P to nonoccluded Po.

2018), and the turnover rate of resin extractable P in Hawaii, United States (>100 g g^{-1} day^{-1}; Helfenstein, Tamburini, et al., 2018), using isotope dilution techniques. These estimates were much higher than our turnover rates of labile P (0.021–0.065 g g^{-1} day^{-1}), because labile P in this study included Fe-impregnated strip extractable P and $NaHCO_3$ extractable Pi, which are both likely to have a slower turnover rate than solution P, and the latter could also have a slower turnover rate than resin extractable P (Hedley et al., 1982; Tiessen & Moir, 2007). Our turnover rates of nonoccluded Po (0.019–0.096 g g^{-1} day^{-1}) were, however, within the range of turnover rate of soil microbial biomass P (MBP) estimated in previous studies using isotope dilution techniques (0.001–0.300 g g^{-1} day^{-1}, recalculated using an MBP concentration of 40 mg/kg if MBP concentration was not given; Achat, Morel, et al., 2010; Bünemann, 2015; Oberson & Joner, 2005), though the nonoccluded Po here probably included both MBP and some other soil organic P compounds (Hou et al., 2016; Tiessen & Moir, 2007). Our turnover rates of secondary mineral P (0.006–0.047 g g^{-1} day^{-1}) and primary mineral P (0.00015–0.00193 g g^{-1} day^{-1}) were comparable to the previous estimates (secondary mineral P: 0.003–0.140 g g^{-1} day^{-1}; primary mineral P: <0.003 g g^{-1} day^{-1}) in Hawaii, United States, which were approximated using a combination of spectroscopic and isotopic techniques (Helfenstein, Tamburini, et al., 2018). These comparisons suggest that our data assimilation approach provides generally comparable estimates of soil P turnover rates with the previous studies using isotopic and spectroscopic techniques.

The turnover rates of the inorganic P pools decreased in the following order: labile P > secondary mineral P > occluded Pi and the turnover rate of nonoccluded Po was faster than that of occluded Po. These results provide empirical support for the hypothesis that the Hedley P fractionation procedure can sequentially extract soil P fractions with decreasing mobility (Hedley et al., 1982; Tiessen et al., 1984; Tiessen & Moir, 2007). Our turnover rates of soil occluded Pi (mean 0.0065 g g^{-1} day^{-1}) and occluded Po (mean 0.0066 g g^{-1} day^{-1}) are the first estimates for the two soil P pools, to the best of our knowledge. These estimates were consistent with some other studies that found a significant change in Hedley occluded P within years or even seasons of plant growth in the field (Fan et al., 2019; Zhang et al., 2006) and suggest that Hedley occluded P is more dynamic than previously thought (i.e., Hedley occluded P is a very stable soil P that is hardly available to plants; Cross & Schlesinger, 1995; Yang et al., 2014). Noted that we estimated soil occluded Pi and occluded Po pools based on soil residual P fraction and *OPo* rather than direct measurements. This may cause some but not large uncertainties in the estimated turnover rates of soil occluded Pi and occluded Po, because the turnover rates of the two P pools were generally comparable across soils and the proportions of occluded P in organic forms (i.e., *OPo*) were generally small for the soils studied (Table 4; Guo et al., 2000).

Beside soil P turnover rates, we have also provided the first estimates of the rates of transformations between all major Hedley P pools. These estimates can convey deep insights into soil P dynamics and soil P bioavailability. For example, the generally larger coefficients of transfer from labile P to secondary mineral P (mean 0.42) and to nonoccluded Po (0.38) than to plants (0.20) suggest that soil secondary minerals and microbes were more competitive than plants in acquiring P from soil labile pool. Nevertheless, since secondary mineral P and nonoccluded Po can be essentially transform back to labile P, their amounts generally decreased while accumulated plant P uptake gradually increased with cropping. Both the coefficient of transfer from labile P to plants and the labile P turnover rate differed between the soils (Table 4), suggesting the varied dynamics of labile P for various soils. These results explain why the amount of labile P has frequently failed to indicate soil P bioavailability (Tandy et al., 2011; Zehetner et al., 2018), as soil P bioavailability is determined not only by the amount and but also by the dynamics of labile P in the soil.

The negative relationship between the coefficients of transfer from labile P to plants and to secondary mineral P suggests a significant competition for P between plants and soil secondary minerals. Significant

relationships between these two parameters and both soil pH and organic C concentration (Figure 3) suggest the regulation of soil pH and organic C concentration on such a competition. It is reasonable to observe an increase in the coefficient of transfer from labile P to secondary mineral P with decreasing soil pH. This is because soil P sorption capacity typically increases with decreasing soil pH (Barrow, 1983; Celi & Barberis, 2005), which also explains the decreasing secondary mineral P turnover rate with decreasing soil pH (Figure 3a). The decrease in the coefficient of transfer from labile P to plants with increasing soil organic C was probably because of an enhancement of microbial P immobilization by soil organic C (Olander & Vitousek, 2004), which can result in a less flow of P from soil labile pool to plants. This hypothesis was supported by the significant and negative relationship between plant P uptake and the coefficient of transfer from labile P to nonoccluded Po (Figure 4).

4.2. Performance and Application of the Data Assimilation System

Our data assimilation system simulated generally well the temporal changes in all the P pools of all the soils studied. The relatively poor simulation of nonoccluded Po was probably due to its relatively large measurement errors (Guo et al., 2000) and highly dynamic nature (George et al., 2018). Theoretically, primary mineral P decreases with plant growth all the time (Vitousek et al., 2010; Walker & Syers, 1976). However, the HCl-P fraction that serves as an index for the amount of primary mineral P increased with cropping in the five highly weathered soils (Figure 1e), probably because they were significantly contaminated by the previous extract (i.e., the NaOH extract; Tiessen & Moir, 2007). This pattern was not well simulated in our study, because as in previous models (e.g., Tiessen et al., 1984), our SPD model did not include any input into primary mineral P.

Beside the soil P turnover rates and transfer coeffecients, our data assimilation system also provided information about the data sets and the model in three other aspects. First, we showed how model parameters were constrained by the available data sets. Here all the parameters describing soil P dynamics were approximately constrained by the 426-day changes in the soil P fractions. This may be a surprise to many scientists, because soil chronosequence studies have found dramatic changes in the major soil P pools in natural terrestrial ecosystems only at timescales of hundreds of years or longer (Vitousek et al., 2010; Walker & Syers, 1976). We proposed two explanations for the seemingly contradictory results. One is that soil chronosequence studies have revealed the net change rates rather than the turnover rates of soil P pools. In fact, the size of a soil P pool changes only in a small proportion within one turnover cycle, because of the replenishments from other soil P pools (Figure 1). An exception was the soil primary mineral P, which can be replenished only at a geological time scale. For example, in the present study, only an average of <20% of the labile P was depleted by crop P uptake within one turnover cycle of labile P (an average of 25 days). The other explanation is that our data sets were derived from experiments performed in a greenhouse, where several experimental treatments (e.g., N fertilization) had been made to facilitate intensive crop P uptake (Guo et al., 2000); therefore, our estimated turnover rates could be higher than those in the field. Nevertheless, our approach can be applied in the field if field changes in terrestrial P pools and fluxes are monitored in a frequent and consistent way, although the model structure and the prior parameter ranges will need to be modified according to the field conditions (Guo et al., 2000; Luo et al., 2011).

Second, we found relationships between the parameters describing the soil P dynamics, which probably reflect relationships defined by the model structure, the correlations between the soil P pools, or errors, or any combination of the three (Gao et al., 2011). For example, the labile P turnover rate was positively correlated with the nonoccluded Po turnover rate, probably because part of the nonoccluded Po (i.e., the $NaHCO_3$-Po) was extracted using the same chemical reagent (0.5 M $NaHCO_3$ at pH 8.5) as the labile P (represented by the $NaHCO_3$-Pi).

Finally, we identified the parameters that are important in simulating the temporal change of a soil P pool, which is critical for forecasting soil P amounts (Gao et al., 2011; Huang et al., 2018). For example, we found that the amount of labile P was the most sensitive to its turnover rate, suggesting that its turnover rate is the most important parameter for simulating and forecasting the amount of labile P. The labile P turnover rate depends on the capabilities of the plants and soil microbes to cycle labile P and soil minerals in fixing/releasing labile P, which need to be explored further by models with more comprehensive P cycle processes. Labile P amount was also sensitive to the secondary mineral P turnover rate in four of the highly

weathered soils and to the primary mineral P release rate in two of the three lightly weathered soils. These results suggest that forecasting labile P amount in highly weathered soils should consider the secondary mineral P turnover rate, while forecasting labile P amount in lightly weathered soils should consider the primary mineral P release rate.

While our SPD model performed reasonably well with the eight data sets selected, it was not tested by other independent data sets, due to a lack of similar published data sets. The structure of the SPD model, though theoretically well established (Tiessen et al., 1984), needs to be evaluated with new greenhouse experiments of the kind used in this study and with field measurements of soil P pools before being extensively adopted for other more general modeling activities (e.g., used as a soil P cycle submodel in earth system models). Future data-model fusion work on soil P dynamics or terrestrial P cycle may also use multiple sources of terrestrial P cycle measurements (e.g., litter P production measured in the field and soil phosphatase activities measured in the laboratory), ideally with the incorporation of more comprehensive P cycle processes and C and nitrogen cycles. We expect more data-model fusion work on the terrestrial P cycle in the future that will essentially improve our understanding and predictions of crop production and terrestrial C sequestration under future global change scenarios.

5. Conclusion

By assimilating eight data sets of 426-day changes in soil P fractions into the SPD model developed in the present study, we successfully quantified the dynamics of all major P pools in a variety of soils in a greenhouse environment. The estimated turnover rates of soil P pools were generally comparable to the previous estimates using isotope dilution and/or spectroscopic approaches. A comparison of turnover rates among soil P pools supported the hypothesis that Hedley P fractionation procedure sequentially extracts soil P pools with decreasing mobility. Meanwhile, we found that Hedley occluded P is more dynamic than previously thought. Differing labile P turnover rates and transfer coefficients with different soils explained why labile P amount frequently fails to indicate the bioavailability of soil P. We also identified soil pH and organic C concentration as the key soil properties that regulate the competition for P between plants and soil secondary minerals. Since our SPD model was similar to the soil P submodels in earth system models (Wang et al., 2010; Yang et al., 2014), our estimated parameter values can aid the parameterization of the soil P submodels, so as to improve the predictions concerning terrestrial ecosystems under future global change scenarios. Overall, we suggest that data assimilation can contribute significantly to an improved understanding of soil P dynamics.

Acknowledgments
We thank F. Guo and her colleagues for their data sets used in the present study, Shuang Ma and Zhenggang Du for their discussion, and the Editors and the two anonymous reviewers for their insightful comments that helped to improve this work. This study was financially supported by the National Natural Science Foundation of China (31870464, 31570483, and 41401326), the U.S. Department of Energy (DE-SC00114085), National Science Foundation grant DEB 1655499, U.S. Department of Energy, Terrestrial Ecosystem Sciences grant DE-SC0006982, the subcontracts 4000158404 and 4000161830 from Oak Ridge National Laboratory (ORNL) to the Northern Arizona University, and the Natural Science Foundation of Guangdong Province (2015A030311029). ORNL's work was supported by the U.S. Department of Energy (DOE), Office of Science, Office of Biological and Environmental Research. ORNL is managed by UT-Battelle, LLC, for the U.S. Department of Energy under contract DE-AC05-00OR22725. Data and code used in this study are available at https://figshare.com/articles/A_soil_phosphorus_dynamics_SPD_model/8273816. The authors declare no competing interests. Enqing Hou and Xingjie Lu contributed equally to this work.

References

Achat, D. L., Bakker, M. R., Zeller, B., Pellerin, S., Bienaimé, S., & Morel, C. (2010). Long-term organic phosphorus mineralization in Spodosols under forests and its relation to carbon and nitrogen mineralization. *Soil Biology and Biochemistry*, *42*(9), 1479–1490. https://doi.org/10.1016/j.soilbio.2010.05.020

Achat, D. L., Morel, C., Bakker, M. R., Augusto, L., Pellerin, S., Gallet-Budynek, A., & Gonzalez, M. (2010). Assessing turnover of microbial biomass phosphorus: Combination of an isotopic dilution method with a mass balance model. *Soil Biology and Biochemistry*, *42*(12), 2231–2240. https://doi.org/10.1016/j.soilbio.2010.08.023

Augusto, L., Achat, D. L., Jonard, M., Vidal, D., & Ringeval, B. (2017). Soil parent material-a major driver of plant nutrient limitations in terrestrial ecosystems. *Global Change Biology*, *23*(9), 3808–3824. https://doi.org/10.1111/gcb.13691

Barrow, N. (1983). A mechanistic model for describing the sorption and desorption of phosphate by soil. *Journal of Soil Science*, *34*(4), 733–750. https://doi.org/10.1111/j.1365-2389.1983.tb01068.x

Brooks, S. P., & Gelman, A. (1998). General methods for monitoring convergence of iterative simulations. *Journal of Computational and Graphical Statistics*, *7*(4), 434–455. https://doi.org/10.1080/10618600.1998.10474787

Bünemann, E. K. (2015). Assessment of gross and net mineralization rates of soil organic phosphorus—A review. *Soil Biology and Biochemistry*, *89*, 82–98. https://doi.org/10.1016/j.soilbio.2015.06.026

Celi, L., & Barberis, E. (2005). Abiotic stabilization of organic phosphorus in the environment. In B. L. Turner, E. Frossard, & D. S. Baldwin (Eds.), *Organic phosphorus in the environment*, (pp. 113–132). Wallingford, Oxon (UK): CABI Publishing.

Chen, C. R., Sinaj, S., Condron, L. M., Frossard, E., Sherlock, R. R., & Davis, M. R. (2003). Characterization of phosphorus availability in selected New Zealand grassland soils. *Nutrient Cycling in Agroecosystems*, *65*(1), 89–100. https://doi.org/10.1023/a:1021889207109

Condron, L. M., & Newman, S. (2011). Revisiting the fundamentals of phosphorus fractionation of sediments and soils. *Journal of Soils and Sediments*, *11*(5), 830–840. https://doi.org/10.1007/s11368-011-0363-2

Cross, A. F., & Schlesinger, W. H. (1995). A literature review and evaluation of the Hedley fractionation—Applications to the biogeochemical cycle of soil phosphorus in natural ecosystems. *Geoderma*, *64*(3-4), 197–214. https://doi.org/10.1016/0016-7061(94)00023-4

Fan, Y., Zhong, X., Lin, F., Liu, C., Yang, L., Wang, M., et al. (2019). Responses of soil phosphorus fractions after nitrogen addition in a subtropical forest ecosystem: Insights from decreased Fe and Al oxides and increased plant roots. *Geoderma*, *337*, 246–255. https://doi.org/10.1016/j.geoderma.2018.09.028

Frossard, E., Condron, L. M., Oberson, A., Sinaj, S., & Fardeau, J. C. (2000). Processes governing phosphorus availability in temperate soils. *Journal of Environmental Quality*, *29*(1), 15–23. https://doi.org/10.2134/jeq2000.00472425002900010003x

Gama-Rodrigues, A. C., Sales, M. V. S., Silva, P. S. D., Comerford, N. B., Cropper, W. P., & Gama-Rodrigues, E. F. (2014). An exploratory analysis of phosphorus transformations in tropical soils using structural equation modeling. *Biogeochemistry*, *118*(1-3), 453–469. https://doi.org/10.1007/s10533-013-9946-x

Gao, C., Wang, H., Weng, E., Lakshmivarahan, S., Zhang, Y., & Luo, Y. (2011). Assimilation of multiple data sets with the ensemble Kalman filter to improve forecasts of forest carbon dynamics. *Ecological Applications*, *21*(5), 1461–1473. https://doi.org/10.1890/09-1234.1

George, T. S., Giles, C. D., Menezes-Blackburn, D., Condron, L. M., Gama-Rodrigues, A. C., Jaisi, D., et al. (2018). Organic phosphorus in the terrestrial environment: A perspective on the state of the art and future priorities. *Plant and Soil*, *427*(1-2), 191–208. https://doi.org/10.1007/s11104-017-3391-x

Guo, F., Yost, R. S., Hue, N. V., Evensen, C. I., & Silva, J. A. (2000). Changes in phosphorus fractions in soils under intensive plant growth. *Soil Science Society of America Journal*, *64*(5), 1681–1689. https://doi.org/10.2136/sssaj2000.6451681x

Hastings, W. K. (1970). Monte Carlo sampling methods using Markov chains and their applications. *Biometrika*, *57*(1), 97–109. https://doi.org/10.1093/biomet/57.1.97

Hedley, M., Stewart, J., & Chauhan, B. (1982). Changes in inorganic and organic soil phosphorus fractions induced by cultivation practices and by laboratory incubations. *Soil Science Society of America Journal*, *46*(5), 970–976. https://doi.org/10.2136/sssaj1982.03615995004600050017x

Helfenstein, J., Jegminat, J., McLaren, T. I., & Frossard, E. (2018). Soil solution phosphorus turnover: derivation, interpretation, and insights from a global compilation of isotope exchange kinetic studies. *Biogeosciences*, *15*(1), 105–114. https://doi.org/10.5194/bg-15-105-2018

Helfenstein, J., Tamburini, F., von Sperber, C., Massey, M. S., Pistocchi, C., Chadwick, O. A., et al. (2018). Combining spectroscopic and isotopic techniques gives a dynamic view of phosphorus cycling in soil. *Nature Communications*, *9*(1), 3226. https://doi.org/10.1038/s41467-018-05731-2

Hou, E., Chen, C., Kuang, Y., Zhang, Y., Heenan, M., & Wen, D. (2016). A structural equation model analysis of phosphorus transformations in global unfertilized and uncultivated soils. *Global Biogeochemical Cycles*, *30*, 1300–1309. https://doi.org/10.1002/2016GB005371

Hou, E., Chen, C., Luo, Y., Zhou, G., Kuang, Y., Zhang, Y., et al. (2018). Effects of climate on soil phosphorus cycle and availability in natural terrestrial ecosystems. *Global Change Biology*, *24*(8), 3344–3356. https://doi.org/10.1111/gcb.14093

Hou, E., Tan, X., Heenan, M., & Wen, D. (2018). A global dataset of plant available and unavailable phosphorus in natural soils derived by Hedley method. *Scientific Data*, *5*, 180166. https://doi.org/10.1038/sdata.2018.166

Hou, E., Wen, D., Kuang, Y., Cong, J., Chen, C., He, X., et al. (2018). Soil pH predominantly controls the forms of organic phosphorus in topsoils under natural broadleaved forests along a 2500 km latitudinal gradient. *Geoderma*, *315*, 65–74. https://doi.org/10.1016/j.geoderma.2017.11.041

Huang, Y., Zhu, D., Ciais, P., Guenet, B., Huang, Y., Goll, D. S., et al. (2018). Matrix-based sensitivity assessment of soil organic carbon storage: A case study from the ORCHIDEE-MICT Model. *Journal of Advances in Modeling Earth Systems*, *10*, 1790–1808. https://doi.org/10.1029/2017MS001237

Liang, J., Li, D., Shi, Z., Tiedje, J. M., Zhou, J., Schuur, E. A. G., et al. (2015). Methods for estimating temperature sensitivity of soil organic matter based on incubation data: A comparative evaluation. *Soil Biology and Biochemistry*, *80*, 127–135. https://doi.org/10.1016/j.soilbio.2014.10.005

Luo, Y., Ahlström, A., Allison, S. D., Batjes, N. H., Brovkin, V., Carvalhais, N., et al. (2016). Toward more realistic projections of soil carbon dynamics by Earth system models. *Global Biogeochemical Cycles*, *30*, 40–56. https://doi.org/10.1002/2015GB005239

Luo, Y., Ogle, K., Tucker, C., Fei, S., Gao, C., LaDeau, S., et al. (2011). Ecological forecasting and data assimilation in a data-rich era. *Ecological Applications*, *21*(5), 1429–1442. https://doi.org/10.1890/09-1275.1

Luo, Y., Weng, E., Wu, X., Gao, C., Zhou, X., & Zhang, L. (2009). Parameter identifiability, constraint, and equifinality in data assimilation with ecosystem models. *Ecological Applications*, *19*(3), 571–574. https://doi.org/10.1890/08-0561.1

Murphy, J., & Riley, J. P. (1962). A modified single solution method for the determination of phosphate in natural waters. *Analytica Chimica Acta*, *27*, 31–36. https://doi.org/10.1016/s0003-2670(00)88444-5

Negassa, W., & Leinweber, P. (2009). How does the Hedley sequential phosphorus fractionation reflect impacts of land use and management on soil phosphorus: A review. *Journal of Plant Nutrition and Soil Science*, *172*(3), 305–325. https://doi.org/10.1002/jpln.200800223

Niu, S. L., Luo, Y. Q., Dietze, M. C., Keenan, T. F., Shi, Z., Li, J. W., & Chapin, F. S. (2014). The role of data assimilation in predictive ecology. *Ecosphere*, *5*(5), 1–16. https://doi.org/10.1890/Es13-00273.1

Oberson, A., & Joner, E. J. (2005). Microbial turnover of phosphorus in soil. In B. L. Turner, E. Frossard, & D. S. Baldwin (Eds.), *Organic phosphorus in the environment*, (pp. 133–164). Wallingford, Oxon (UK): CABI Publishing.

Olander, L. P., & Vitousek, P. M. (2004). Biological and geochemical sinks for phosphorus in soil from a wet tropical forest. *Ecosystems*, *7*(4), 404–419. https://doi.org/10.1007/s10021-004-0264-y

Penuelas, J., Poulter, B., Sardans, J., Ciais, P., Van Der Velde, M., Bopp, L., et al. (2013). Human-induced nitrogen-phosphorus imbalances alter natural and managed ecosystems across the globe. *Nature Communications*, *4*(1), 2934. https://doi.org/10.1038/ncomms3934

Reed, S. C., Yang, X., & Thornton, P. E. (2015). Incorporating phosphorus cycling into global modeling efforts: a worthwhile, tractable endeavor. *New Phytologist*, *208*(2), 324–329. https://doi.org/10.1111/nph.13521

Roy, E. D., Richards, P. D., Martinelli, L. A., Coletta, L. D., Lins, S. R. M., Vazquez, F. F., et al. (2016). The phosphorus cost of agricultural intensification in the tropics. *Nature Plants*, *2*(5), 16,043. https://doi.org/10.1038/nplants.2016.43

Sun, Y., Peng, S., Goll, D. S., Ciais, P., Guenet, B., Guimberteau, M., et al. (2017). Diagnosing phosphorus limitations in natural terrestrial ecosystems in carbon cycle models. *Earth's Future*, *5*(7), 730–749. https://doi.org/10.1002/2016ef000472

Tandy, S., Mundus, S., Yngvesson, J., de Bang, T. C., Lombi, E., Schjørring, J. K., & Husted, S. (2011). The use of DGT for prediction of plant available copper, zinc and phosphorus in agricultural soils. *Plant and Soil*, *346*(1-2), 167–180. https://doi.org/10.1007/s11104-011-0806-y

Tiessen, H., & Moir, J. (2007). Characterization of available P by sequential extraction. In M. R. Carter, & E. G. Gregorich (Eds.), *Soil Sampling and Methods of Analysis*, (Second ed.pp. 293–306). CRC Press: Boca Raton, FL.

Tiessen, H., Stewart, J., & Cole, C. (1984). Pathways of phosphorus transformations in soils of differing pedogenesis. *Soil Science Society of America Journal*, *48*(4), 853–858. https://doi.org/10.2136/sssaj1984.03615995004800040031x

Vitousek, P. M., Porder, S., Houlton, B. Z., & Chadwick, O. A. (2010). Terrestrial phosphorus limitation: mechanisms, implications, and nitrogen-phosphorus interactions. *Ecological Applications*, *20*(1), 5–15. https://doi.org/10.1890/08-0127.1

Walker, T. W., & Syers, J. K. (1976). The fate of phosphorus during pedogenesis. *Geoderma*, *15*(1), 1–19. https://doi.org/10.1016/0016-7061(76)90066-5

Wang, Y. P., Law, R. M., & Pak, B. (2010). A global model of carbon, nitrogen and phosphorus cycles for the terrestrial biosphere. *Biogeosciences*, *7*(7), 2261–2282. https://doi.org/10.5194/bg-7-2261-2010

Yang, X., Thornton, P. E., Ricciuto, D. M., & Post, W. M. (2014). The role of phosphorus dynamics in tropical forests—A modeling study using CLM-CNP. *Biogeosciences*, *11*(6), 1667–1681. https://doi.org/10.5194/bg-11-1667-2014

Zehetner, F., Wuenscher, R., Peticzka, R., & Unterfrauner, H. (2018). Correlation of extractable soil phosphorus (P) with plant P uptake: 14 extraction methods applied to 50 agricultural soils from Central Europe. *Plant, Soil and Environment*, *64*(4), 192–201. https://doi.org/10.17221/70/2018-PSE

Zhang, Q., Wang, G. H., Feng, Y. K., Sun, Q. Z., Witt, C., & Dobermann, A. (2006). Changes in soil phosphorus fractions in a calcareous paddy soil under intensive rice cropping. *Plant and Soil*, *288*(1-2), 141–154. https://doi.org/10.1007/s11104-006-9100-9